

Stabilisation of a short α -helical VIP fragment by side chain to side chain cyclisation: a comparison of common cyclisation motifs by circular dichroism

Lukasz Frankiewicz,^{a†} Cecilia Betti,^{a†} Karel Guillemyn,^a Dirk Tourwé,^a Yves Jacquot^{b*} and Steven Ballet^{a*}

A model octapeptide segment derived from vasoactive intestinal peptide (VIP) was utilised to investigate the effect of several conventional cyclisation methods on the α -helical conformation in short peptide fragments. Three of the classical macrocyclisation techniques (i.e. lactamisation, ring-closing metathesis and Huisgen cycloaddition) were applied, and the conformations of the resulting cyclic peptides, as well as their linear precursors, were compared by CD analysis. The visibly higher folding propensity of the triazole-tethered peptide after azide-alkyne CuAAC macrocyclisation illustrates that the secondary structure of a short peptide fragment can differ significantly depending on the chemical strategy used to covalently cross-link side chain residues in a 'helical' fragment. Copyright © 2013 European Peptide Society and John Wiley & Sons, Ltd.

Keywords: Helix stabilisation; circular dichroism; cyclisation motifs; macrolactamisation; ring-closing metathesis; Huisgen cycloaddition

Introduction

Because the recognition of peptide ligands by their respective receptor proteins often occurs at the level of well-structured secondary helical or turn domains [1], all synthetic methodologies that enable peptides to adopt a specific secondary structure are of interest for peptide-based drug development. Classically, after the identification of the so-called hot spot contacts and the establishment of the pharmacophore, medicinal chemists attempt to stabilise the appropriate 'bioactive' conformation. To realise this, an important design feature consists of stabilising the key amino acid side chains in the suited topographical orientation for interaction with the protein, as they contribute significantly to the binding energy [2].

The revival of synthetic peptides, especially cyclic ones, as potential therapeutic candidates [3–5], is a consequence of the combination of different, related, aspects as follows: (i) cyclopeptides show a superior resistance to endopeptidase and exopeptidase, as compared with linear peptides, (ii) a reduction in molecular flexibility generally yields more potent and target-selective peptide ligands, and (iii) recent advances in the synthesis, delivery and formulation of peptides have been made [3].

It is now also documented that cyclic peptides are suitable for extended interactions, such as the ones needed for previously believed 'undruggable' protein–protein interactions (PPIs) [6]. Because of the large interaction surfaces that are characteristic of these PPIs, it is cumbersome to address these difficult targets with low-molecular weight compounds.

More specifically, α -helical subdomains of proteins often serve as recognition motifs for PPIs, but when taken out of their tertiary structure, the peptide fragments that constitute these subdomains

adopt little, if any, α -helical structure [7]. For this reason, synthetic techniques or methodologies that stabilise or mimic helical conformations have received considerable attention over the past decade [8,9]. Next to the development of promising non-peptide mimetics and modified peptide backbones that mimic the properties of α -helices, examples of side-chain cross-linked peptides with remarkable biological activities have been reported. The 'stapled peptide' technology, which is based on RCM reactions of modified, olefin-containing residues, has resulted in unprecedented results in, for example, stabilised α -helical peptides from the human B-cell lymphoma-2 (Bcl-2) family of proteins and their therapeutic use for controlling cell death events [10]. The increased

* Correspondence to: Steven Ballet, Organic Chemistry Department, Vrije Universiteit Brussel, Pleinlaan 2, B-1050 Brussels, Belgium. E-mail: sballet@vub.ac.be
Yves Jacquot, Department of Chemistry, Ecole Normale Supérieure, 24, rue Lhomond, 75231 Paris Cedex 05, France. E-mail: yves.jacquot@upmc.fr

† Authors contributed equally to this work.

a Department of Organic Chemistry, Vrije Universiteit Brussel, Pleinlaan 2, B-1050, Brussels, Belgium

b Laboratory of the BioMolécules (LBM), Department of Chemistry, CNRS - UMR 7203, Ecole Normale Supérieure/Université Pierre et Marie Curie Paris 6, 24, rue Lhomond, 75231, Paris Cedex 05, France

Abbreviations: Aib, 2-amino-2-methylpropanoic acid; All, allyl; Alloc, allyloxycarbonyl; CD, circular dichroism; DIPEA, *N,N*-diisopropylethylamine; DMF, *N,N*-dimethylformamide; HCTU, 2-(6-chloro-1H-benzotriazole-1-yl)-1,3,3-tetramethylammonium hexafluorophosphate; MRE, maximum mean residue ellipticity; Nle, norleucine; Pra, propargylglycine; RCM, ring-closing metathesis; SPPS, solid-phase peptide synthesis; TBTU, *O*-(benzotriazol-1-yl)-*N,N,N',N'*-tetramethyluronium tetrafluoroborate; TFE, 2,2,2-trifluoroethanol; VIP, vasoactive intestinal peptide.

cell permeability of stapled peptides has also made them interesting compounds for targeting intracellular drug targets [11]. A second reported strategy to achieve the same goal, that is, obtaining enhanced helical structure, consists of linking the *i* and *i*+4 side chains in a peptide via a Cu-catalysed intramolecular Huisgen azide–alkyne cycloaddition reaction (CuAAC) [12,13]. From the work of Scrima *et al.*, it was concluded that the number of methylene units present in the side chain bridge, which determine the length of the cross-link, are important for helicity. Whereas ‘long’ (seven CH₂ groups) and ‘short’ (four CH₂ groups) linkers did not stabilise the helical structure, bridged peptides in which the triazole was flanked by five or six methylene units (corresponding to an 8-atom or 9-atom tether, respectively) nicely accommodated the desired helix. Triazole-stapling has recently been used for the stabilisation of B-cell CLL/lymphoma 9 (BCL9) α -helical peptides [14]. This study, comprising single and double triazole-bridged analogues, aimed at improved BCL9 – β -catenin binding for blockade of the transcriptional activity of β -catenin, to suppress the tumorigenesis of several types of human cancer. When using triazole bridges, Kawamoto and coworkers showed that a 7-atom linker was not suited for optimal binding recognition, confirming short triazole linkers to be inadequate for their purpose. In contrast, this linker length was reported to be suited for stabilising constrained nociceptin derivatives by *i* – *i*+4 amide bond formation (‘lactamisation’) using the side chain functionalities of Asp at position *i* and Lys at *i*+4 [15].

The idea of stabilising helices through cross-linkage of a single turn of the helical peptide domain by RCM was launched and realised by Grubbs [16]. Through the use of *O*-allyl serine residues, located on adjacent helical turns, a tether was installed between the *i* and *i*+4 residue side chains in a helical model heptapeptide after RCM conditions were applied.

In a later stage, Verdine and coworkers determined and fine-tuned the requirements that were important for both *i* – *i*+4 and *i* – *i*+7 tethers [17]. When using olefin-containing all-hydrocarbon (but α,α -disubstituted) (*S*)-amino acids, they observed that linkers of 7 or 8 atoms were required.

In this study, a model octapeptide segment, derived from vasoactive intestinal peptide (VIP), was utilised to verify the effect of several conventional cyclisation methods on the α -helical conformation in short peptide fragments. This helical conformation is characterised for more than half of the complete 28-amino acid long VIP sequence **1** [18]. It was reported that a C-terminal truncation of the VIP peptide results in a loss of helicity and a concomitant drop in bioactivity [18]. Because this feature is common in α -helical peptides, that is, a decreased helicity upon truncation and taking into account that one of the classic steps in the peptide-to-drug process consists of identifying the shortest fragment with retained activity, we have taken the central VIP (15–22) (fragment **2** in Table 1) and submitted it to different side chain to side chain macrocyclisations. Three of the classical

Table 1. Peptide sequences of VIP **1** and model peptide **2** [18]

Compound	Peptide sequence*
VIP 1	H-His ¹ -Ser-Asp-Ala-Val-Phe-Thr-Asp-Asn-Tyr-Thr-Arg-Leu-Arg-Lys-Gln-Met-Ala-Val-Lys-Lys-Tyr-Leu-Asn-Ser-Ile-Leu-Asn ²⁸ -NH ₂
Fragment 2	H-Lys ¹⁵ -Gln-Met-Ala-Val-Lys-Lys-Tyr ²² -NH ₂

* The underlined amino acids are part of an α -helical region.

macrocyclisation techniques (i.e. amide bond formation or lactamisation, RCM and triazole ‘click’) were employed, taking into account the aforementioned criteria related to appropriate linker length for *i* – *i*+4 bridging. The propensity of each macrocyclic linkage to stabilise the helical secondary structure (Figure 1) was investigated by circular dichroism.

Materials and Methods

General. Mass spectrometry was recorded on a Micromass Q-TOF spectrometer using electrospray ionisation (positive or negative ion mode). Data collection was performed with Masslynx software. Analytical RP-HPLC was performed using an Agilent 1100 Series system (Waldbronn, Germany) with a Supelco Discovery BIO Wide Pore[®] (Bellefonte, PA, USA) RP C-18 column (25 cm \times 4.6 mm, 5 μ m) using UV detection at 215 nm. The mobile phase (water/acetonitrile) contained 0.1% TFA. The standard gradient consisted of a 20-min run from 3% to 97% acetonitrile at a flow rate of 1 ml min⁻¹. Preparative HPLC was performed on a Gilson apparatus (Gilson, Inc., WI, USA) and controlled with the software package Unipoint. The reversed phase C18-column (Discovery BIO Wide Pore 25 cm \times 21.2 mm, 10 μ m) was used under the same conditions as the analytical RP-HPLC but with a flow rate of 20 ml min⁻¹. A purity of more than 95% was determined for all compounds by analytical RP-HPLC using the conditions described in the succeeding text.

Peptide Synthesis

A. Linear Peptides

The linear peptides **2**, **3**, **4**, **5**, **9** (Table 2) were synthesised via standard solid-phase peptide synthesis using Rink amide resin as the solid support (169 mg, 0.1 mmol, 0.59 mmol g⁻¹). N^z-Fmoc chemistry was applied, and the coupling reactions were performed with 4 eq of amino acid, 4 eq of HCTU and *N*-methylmorpholine in DMF. Removal of the Fmoc protecting group was realised by means of 20% 4-methylpiperidine in DMF (5 min, then again for 15 min). Once the sequence was completed, the resin was treated with a mixture of TFA/H₂O/anisole 95:2.5:2.5 v/v for 3 h in order to cleave the peptide from the resin and to remove the side chain protecting groups. After precipitation in cold diethylether and drying, the crude peptides were purified by preparative RP-HPLC.

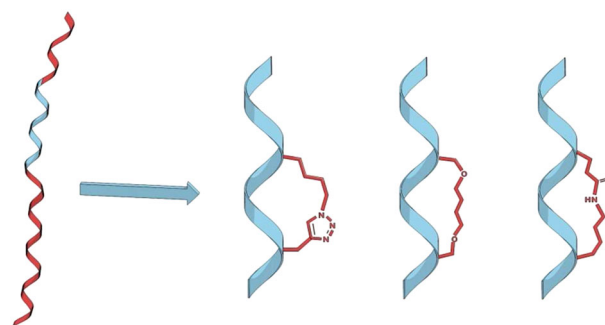
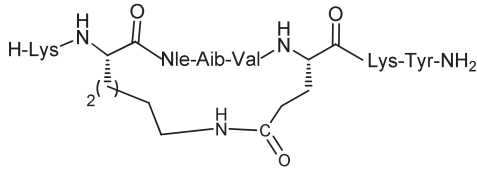
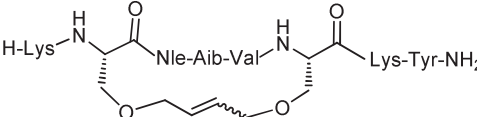
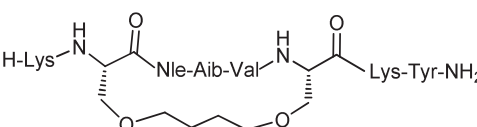
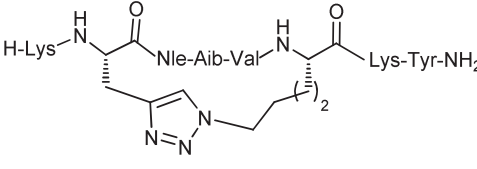


Figure 1. Schematic representation of a full helical sequence (left) and stabilisation of helical conformation in a fragment (blue) by Huisgen azide–alkyne cycloaddition, RCM and amide bond formation (right).

Table 2. Peptide sequences and compound numbers

Sequence	Compound number
H-Lys ¹ -Gln-Met-Ala-Val-Lys-Lys-Tyr ⁸ -NH ₂	2
H-Lys ¹ -Gln-Nle-Aib-Val-Lys-Lys-Tyr ⁸ -NH ₂	3
H-Lys-Gln-Nle-Aib-Val-Lys-Lys-NH ₂	4
H-Lys-Gln-Nle-Aib-Val-Lys-Lys-Ala-NH ₂	5
	6
	7
	8
H-Lys-Pra-Nle-Aib-Val-ε-N ₃ Lys-Lys-Tyr-NH ₂	9
	10

Peptide characterisation. **H-Lys-Gln-Met-Ala-Val-Lys-Lys-Tyr-NH₂ 2 (VIP 15-22)**: HPLC (standard gradient): t_{ret} = 8.00 min. ESI-HRMS [M + H⁺]: m/z = 994.5612 (calculated for C₄₅H₇₉H⁺N₁₃O₁₀S: 994.5794)

H-Lys-Gln-Nle-Aib-Val-Lys-Lys-Tyr-NH₂ 3: HPLC: t_{ret} = 7.99 min. ESI-HRMS [M + H⁺]: m/z = 990.6300 (calculated for C₄₇H₈₃H⁺N₁₃O₁₀: 990.6386)

H-Lys-Gln-Nle-Aib-Val-Lys-Lys-NH₂ 4: HPLC (standard gradient): t_{ret} = 7.86 min.; ESI-HRMS [M + H⁺]: m/z = 827.5800 (calculated for C₃₈H₇₄H⁺N₁₂O₈: 827.5753)

H-Lys-Gln-Nle-Aib-Val-Lys-Lys-Ala-NH₂ 5: HPLC (standard gradient): t_{ret} = 7.87 min.; ESI-HRMS [M + H⁺]: m/z = 898.5920 (calculated for C₄₁H₇₉H⁺N₁₃O₉: 898.6124)

H-Lys-Pra-Nle-Aib-Val-ε-N₃Lys-Lys-Tyr-NH₂ 9: HPLC (standard gradient): t_{ret} = 10.71 min.; ESI-HRMS [M + H⁺]: m/z = 983.6005 (calculated for C₄₇H₇₈H⁺N₁₄O₉: 983.6076).

B. Cyclic Peptides

Synthesis of H-Lys-c[Lys-Nle-Aib-Val-Glu]-Lys-Tyr-NH₂ 6

The resin-bound linear precursor Fmoc-Lys(Boc)-Lys(Alloc)-Nle-Aib-Val-Glu(All)-Lys(Boc)-Tyr(tBu)-Rink amide resin was prepared following the general procedure (0.1 mmol scale). Alloc.../All protecting groups were selectively removed with a solution of

phenylsilane (24 eq) and tetrakis(triphenylphosphine)-palladium (0) (0.2 eq) in dry DCM (2 times 15 min, r.t.). The cyclisation was performed overnight on resin by use of 4 eq HCTU and 8 eq of DIPEA in DMF. Completion of the cyclisation was verified by the Kaiser test. Removal of the terminal Fmoc protecting group, cleavage of the peptide from the resin and concomitant side chain protecting group removal were followed by final purification as described earlier. HPLC (standard gradient): t_{ret} = 9.21 min.; ESI-HRMS [M + H⁺]: m/z = 973.5944 (calculated for C₄₇H₈₀H⁺N₁₂O₁₀: 973.6120).

Synthesis of compounds 7 and 8

Fmoc-Lys(Boc)-Ser(All)-Nle-Aib-Val-Ser(All)-Lys(Boc)-Tyr(tBu)-NH₂ was synthesised according to the general SPPS protocol (0.1 mmol scale). The peptide-resin was subsequently dried for 3 h and swollen in 3 ml of degassed 1,2-dichloroethane under argon atmosphere for 30 min in a round-bottom flask. Next, the Hoveyda-Grubbs catalyst (20 mg in 3 ml of degassed 1,2-dichloroethane) was added, and the mixture was stirred overnight at 50 °C. Intermediate small scale cleavage indicated incomplete conversion and hence, a second portion of catalyst was added, and the mixture was stirred for an additional 2 h. Fmoc removal, cleavage from the resin and purification yielded the pure CH₂CHCH₂-tethered peptide **7**. Finally, in order to obtain the saturated linker in **8**, compound **7** was reduced in MeOH solution by means of 10% Pd/C (10% (w/w)) under H₂ atmosphere (20 psi, r.t.) for 3 h. The crude peptide was again purified as described in the general method.

H-Lys-c[Ser(CH₂CH=)-Nle-Aib-Val-Ser(CH₂CH=)]-Lys-Tyr-NH₂ 7. HPLC (standard gradient): t_{ret} = 10.71 min.; ESI-HRMS [M + H⁺]: m/z = 961.1655 (calculated for C₄₆H₇₇H⁺N₁₁O₁₁: 961.1707)

H-Lys-c[Ser(CH₂CH₂)-Nle-Aib-Val-Ser(CH₂CH₂)]-Lys-Tyr-NH₂ 8. HPLC (standard gradient): t_{ret} = 10.31 min.; ESI-HRMS [M + H⁺]: m/z = 963.1855 (calculated for C₄₆H₇₉H⁺N₁₁O₁₁: 963.1866).

Synthesis of compound 10

In solution: Compound **9** (0.008 mmol, 10 mg) was dissolved in 10 ml tBuOH/H₂O (1:1 v/v) and 6 eq of sodium ascorbate (6 eq, 0.048 mmol, 9 mg) and 4 eq of CuSO₄·5H₂O (4 eq, 0.032 mmol, 8 mg) were added. The reaction mixture was stirred overnight at room temperature. After full conversion (HPLC monitoring), the crude cyclised peptide was purified as described in the general method.

On solid support. The protected peptide Fmoc-Pra-Nle-Aib-Val-ε-N₃Nle-Lys(Boc)-Tyr(tBu)-NH-Rink was synthesised following the general procedure (0.05 mmol scale), and the cyclisation was carried out as follows: the resin was swollen in DMF, and sodium ascorbate (2 eq, 0.1 mmol, 20 mg), CuI (2 eq, 0.1 mmol, 19 mg) and DIPEA (3 eq, 0.15 mmol, 25 μl) were added. The mixture was shaken overnight, filtered, and the resin was washed three times with DMF, iPrOH, DCM and finally five times (5 ml) with a sodium diethyl dithiocarbamate/DIPEA solution in DMF (50 mg/25 μl in 25 ml). After Fmoc removal, the final Lys residue was coupled by addition of N^z-Boc-Lys(Boc)-OH·DCHA (3 eq, 0.15 mmol, 79 mg), TBTU (3 eq, 0.15 mmol, 48 mg) and DIPEA (9 eq, 0.45 mmol, 74 μl) in DMF. Standard coupling of 90 min was followed by washing steps and peptide cleavage and purification.

HPLC (standard gradient): t_{ret} = 9.58 min.; ESI-HRMS [M + H⁺]: m/z = 983.5830 (calculated for C₄₇H₇₈H⁺N₁₄O₉: 983.6076)

Circular Dichroism

Circular dichroism spectra were recorded with a Jobin Yvon CD6 (Jobin Yvon Horiba, Longjumeau, France) apparatus by using a 250 μl (1 mm path length) quartz cell. Each peptide was dissolved in 18.2 M Ω deionized water (milliQ, Millipore) alone or with various amounts of 2,2,2-trifluoroethanol (TFE) at a concentration of 50 μM . Prior to recording, each sample was allowed to equilibrate for 5 min at different temperatures (5, 15, 20, 25, 35, 40, 45 and 55 $^{\circ}\text{C}$) or in various water/TFE mixtures (0, 10, 20, 30, 40, 50 or 60% TFE in water). Absorbance differences were recorded at 1 nm interval (1 s integration time) from 190 to 260 nm and were averaged over four scans. After solvent subtraction, smoothing and baseline correction, absorbance data were treated by using the Dichrograph Software version 1.2 and converted into mean residue molar circular dichroism $\Delta\epsilon$ (in $\text{M}^{-1} \text{cm}^{-1}$) following the equation $\Delta\epsilon = (\Delta A/lc)/n$, where l corresponds to the cell path length (in cm), c corresponds to the peptide concentration (in M) and n to the number of residues. Then, $\Delta\epsilon$ values were converted into mean residue molar ellipticity $[\theta]$, in $10^{-3} \text{deg cm}^2 \text{dmol}^{-1}$ from the equation $[\theta] = 3.298 \Delta\epsilon$.

Results and Discussion

Several strategies are available for the stabilisation of the most abundant protein secondary structure in nature, the α -helix, and comprise both covalent and non-covalent (e.g. electrostatic and metal complexation) stabilisation [8]. During the last decade, the covalent stabilisation by a side chain to side chain tether has become a common technique to stabilise helical and turn conformations of promising, bioactive peptide segments. However, these stabilisation techniques have rarely been applied to the same peptide in order to verify which technique might be the most suited for fixing the desired helical form. Different cyclisation motifs were however compared in a recent study that aimed at mimicking the β -turn structure of tendamistat [19]. Next to the conventional disulfide-bridged and backbone-cyclised lactam cyclopeptide analogues, the triazole-cyclised and linear β^3 and/or β^2 -amino acid-containing peptides were checked for their propensity to induce a β -turn conformation. This comparative study demonstrated that the Huisgen cycloaddition (formation of triazole) and linear β -amino acid-containing peptides (e.g. with inclusion of β^3 homo-amino acids or the turn-inducing β^2 - β^3 dipeptide motif) [20] were not giving way to the desired β -turn stabilisation. This is in contrast to the linear and backbone 'lactamised' and to a lesser extent, the disulfide-bridged analogues, which seemed to readily adopt the folded structure in solution [19].

Herein, and along the same line of the aforementioned study, the propensity of cyclised peptides as well as of their linear precursors (Table 2) to adopt a helical conformation was investigated using CD, a powerful method for exploring the secondary structure of peptides.

For the study of the conformational state of a bioactive compound, which is relevant to the one in its natural environment, water seemed to be the most appropriate medium. However, because of its high polarity and its propensity to create intermolecular hydrogen bonds, it is a poorly structuring solvent. For this reason, our spectroscopic studies were carried out in water with 2,2,2-trifluoroethanol (TFE, 0 \rightarrow 60% v/v). Similarly to CHCl_3 , TFE promotes peptide folding, allowing access to secondary structures (i.e. mainly helix [21,22] or to a lesser extent

β -forms [23] such as hairpin and turns). The mechanisms by which TFE induces the structural organisation of peptides are not entirely resolved. It may occur (i) through direct association with the peptide of interest [24], (ii) by limiting H_2O -peptide interactions [25], (iii) by favouring the formation of $-\text{C}=\text{O}\cdots\text{HN}-$ intramolecular H-bonds [25] and (iv) by increasing the viscosity of the medium (density of TFE 1.391). The folding kinetics of the open and cyclised peptides in 50% TFE was studied by recording CD spectra as a function of the percentage of TFE (0, 10, 20, 30, 40, 50 and 60). Likewise, the conformational stability was investigated as a function of the temperature of the medium (5, 15, 25, 35, 45 and 55 $^{\circ}\text{C}$).

Linear Peptides

First, we determined the spectroscopic signature of the wild-type peptide fragment VIP (15–22) (H-Lys¹-Gln-Met-Ala-Val-Lys-Lys-Tyr⁸-NH₂ **2**, Table 2).

Because of the presence of a phenolic chromophore at the side chain of the C-terminal Tyr⁸ in **2**, an absorbance band that is not correlated to the polypeptide backbone conformation may appear. In fact, this phenomenon occurs when the flexibility of the aromatic amino acid side chains (tryptophan, tyrosine and phenylalanine) is restricted around χ_1 dihedral angles, encouraging chirality. The phenol of the tyrosine is usually characterised by three absorption bands that are associated with $\pi\pi^*$ transitions: at 190 nm (B_a and B_b transition states), 230 nm (L_a transition state) and 280 nm (L_b transition state), following Platt's nomenclature [26–29].

In the case of the peptide **2**, no absorption band ascribed to the phenol of Tyr⁸ was observed (spectrum recorded from 180 to 380 nm, data not shown). Thus, we assumed that the CD spectra of this peptide and of those explored in the present study will exclusively reflect the spatial orientation of the backbone. Likewise, any potential influences of the modified amino acid side chains on the overall peptide conformation was verified by recording the CD spectrum of an initial set of linear peptides in a large wavelength range (from 180 to 380 nm) in water alone and at 25 $^{\circ}\text{C}$. The CD signatures of VIP fragment **2**, its analogue **3** (H-Lys-Gln-Nle-Aib-Val-Lys-Lys-Tyr-NH₂) and the peptides H-Lys-Gln-Nle-Aib-Val-Lys-Lys-NH₂ (compound **4**) and H-Lys-Gln-Nle-Aib-Val-Lys-Lys-Ala-NH₂, (compound **5**), corresponding to fragment **3** devoid of the C-terminal tyrosine or bearing an alanine instead of a tyrosine, respectively, were recorded and displayed similar spectroscopic profiles. These results confirmed the absence of any tyrosine-induced chromophoric effect [Figure 2(A)].

In water, compound **2** displays a CD signature relevant to a random form with a strong negative maximum at 194 nm $[\theta] = -27\,253 \text{ deg cm}^2 \text{dmol}^{-1}$, $\pi\pi^*$ transition, Figure 2(A)]. Because of medium change, this band is slightly red-shifted at 199 nm $[\theta] = -9839 \text{ deg cm}^2 \text{dmol}^{-1}$ in 50% TFE [Figure 2 (B)]. Thus, random populations predominate, even in structuring conditions. In 50% TFE, analogues **4** (without Tyr⁸) and **5** (Tyr⁸ \rightarrow Ala⁸) behave differently than the 'native' VIP fragment (but with Met³ \rightarrow Nle³ substitution, compound **3**), suggesting that the C-terminal tyrosine participates, even modestly, to peptide folding [Figure 2(B)].

The peptide analogue which was used as a reference in this study, that is, compound **3**, resulted from the well-established Met to Nle substitution to avoid an anticipated Met³ side chain

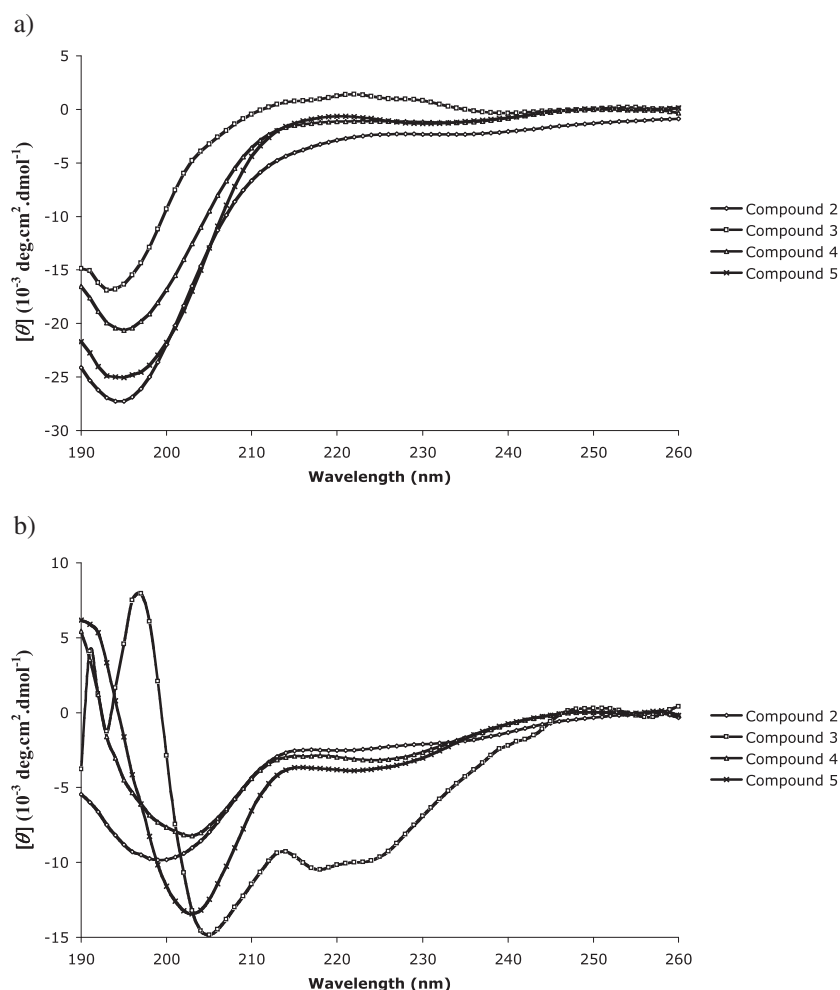


Figure 2. CD spectra of the linear peptides **2**, **3**, **4** and **5** at 50 μM and at 25 $^{\circ}\text{C}$ (a) in water and (b) in 50% TFE. The mean residue ellipticity $[\theta]$ values are expressed in $10^{-3} \text{ deg cm}^2 \text{ dmol}^{-1}$.

oxidation and from the observation that H-Lys-Gln-Nle-Ala-Val-Lys-Lys-Tyr-NH₂ peptide (i.e. [Ala⁴]-**3**) did not cyclise efficiently under the applied RCM conditions (hence, the substitution to Aib, see later discussion of RCM peptides **7** and **8**). Aib is a well-established inducer of 3₁₀ helices [30–32] and is often introduced to make a sequence prone to folding. Looking more closely at compound **3** in water alone and at 25 $^{\circ}\text{C}$, this peptide is characterised by a negative maximum at 193 nm [$[\theta] = -16\,898 \text{ deg cm}^2 \text{ dmol}^{-1}$], revealing the presence of random statistical-coil conformation states [Figure 3(A)]. In a 50% TFE in water medium [Figure 3(A)], this $\pi\pi^*$ transition is of lower intensity and red-shifted to 205 nm [$[\theta] = -14\,830 \text{ deg cm}^2 \text{ dmol}^{-1}$], an observation that can be caused by the medium or to some folding events. Because of the additional positive maximum recorded at 197 nm [$[\theta] = 7947 \text{ deg cm}^2 \text{ dmol}^{-1}$] and the local negative shoulder at ~ 220 nm [$[\theta] = -10\,477 \text{ deg cm}^2 \text{ dmol}^{-1}$], helix structure is likely. The fact that the intensity of the band at ~ 220 nm is smaller to the one at 205 nm suggests the formation of a 3₁₀ helix, confirming the role of Aib in this context [33,34]. It is noteworthy that the low intensity of the band at 197 nm is also in favour of 3₁₀ helix [16,35,36]. However, 11 and 14/15-helix (i.e. α/β -mixed peptides) is not totally excluded [37,38].

In Figure 4(A), the CD spectra of the wild-type peptide **2** in different concentrations of TFE are shown. The graph insets

represent the evolution of the intensity of the negative maximum at ~ 205 nm as a function of the percentage of TFE. Such a graph is informative regarding the propensity of a given peptide to adopt a regular structure. In this regard, it should be stressed that for all the studied peptides, the evolution of the intensity of the negative maximum at ~ 222 nm (data not shown) correlated to that recorded at ~ 205 nm. When recording CD profiles as a function of an incremental concentration of TFE (v/v), a limited decrease of the intensity of the negative band at ~ 205 nm for compound **2** was observed, confirming not only that the peptide adopts a more regular structure when TFE concentration increases but also that the random states participate in the absorbance recorded at this wavelength [Figure 4(A)]. Note that a red-shift (from 195 to 220 nm) is observed, allowing to consider two conformational populations, depending on the percentage of TFE: the populations where the band is at 185 nm would be relevant to random populations, whereas those that share a band at 200 nm are relevant to structured populations.

Cyclised Peptides

The conformational effects resulting from different side chain to side chain cyclisation strategies were explored and placed in perspective

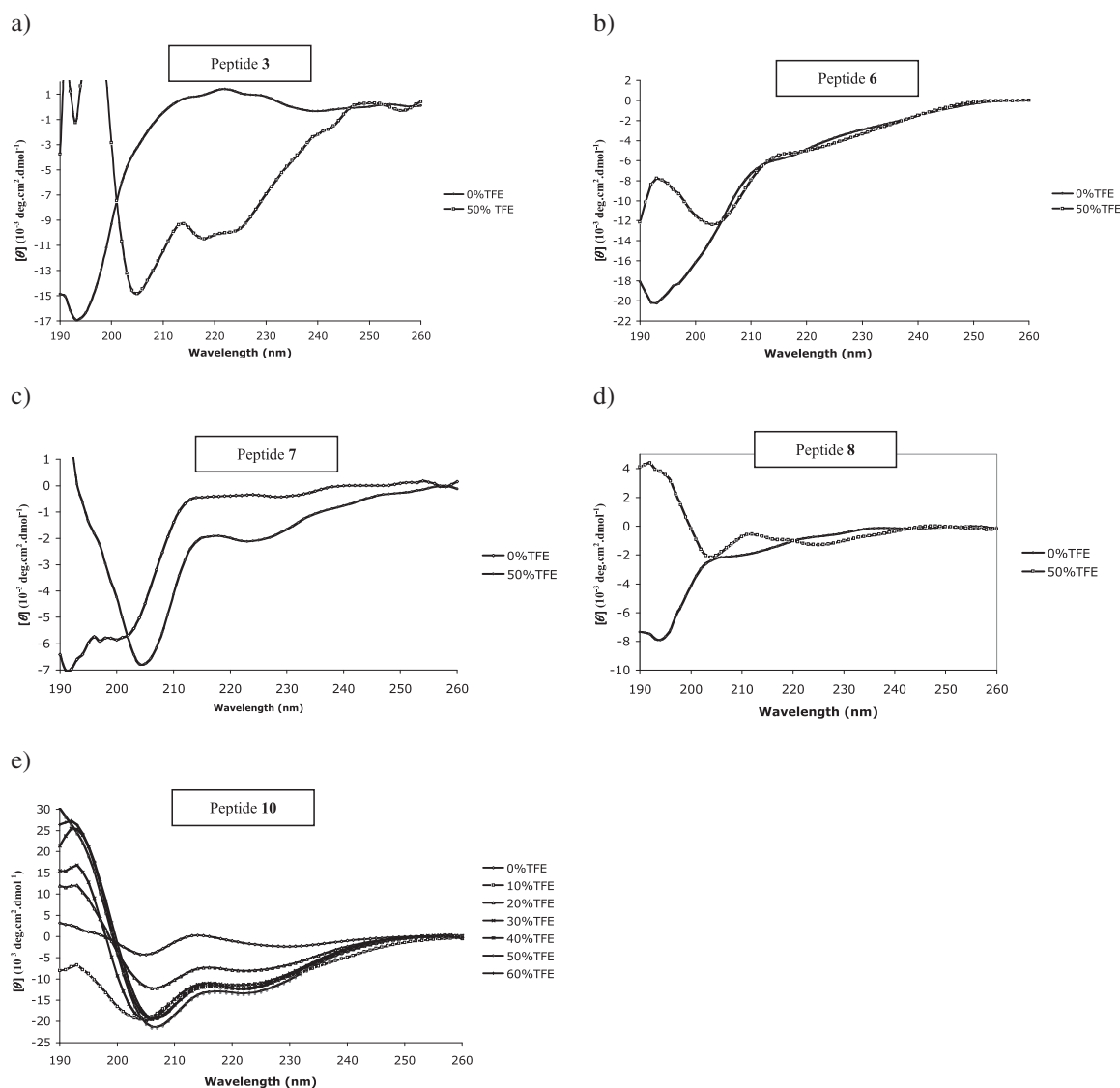


Figure 3. CD spectra of the synthesised peptides at a concentration of 50 μM in water alone or in water with 50% TFE, at 25 $^{\circ}\text{C}$. (a) Peptide **3**, (b) peptide **6**, (c) peptide **7**, (d) peptide **8** and (e) peptide **10**. The mean residue ellipticity $[\theta]$ values are expressed in 10^{-3} $\text{deg cm}^2 \text{dmol}^{-1}$.

with earlier studies, such as those of Scrima [12] and Kawamoto [14]. Aside from disulphide bridge formation, the most commonly utilised cyclisation techniques were directly compared in this work and involved lactamisation, RCM and Cu-catalysed Huisgen cycloaddition (CuAAC) reactions.

A macrocyclic amide analogue of reference peptide **3**, that is, H-Lys-c[Lys-Nle-Aib-Val-Glu]-Lys-Tyr-NH₂ (peptide **6**), was prepared and its CD signature was recorded. The applied cyclisation conditions (HCTU/DIPEA in DMF for 4 h) did not allow the i to i + 4 side chain to side chain cyclisation for the synthesis of the c[Glu², Lys⁶]-analogue. As a consequence, this latter analogue was not included in the present study.

In peptide **6**, the amide bond formation between the residues i (Lys²) and i + 4 (Glu⁶) induces a negative absorption band relevant to a random state at 193 nm [$[\theta] = -20,255 \text{ deg cm}^2 \text{dmol}^{-1}$, $\pi\pi^*$ transition], in water at 25 $^{\circ}\text{C}$ [Figure 3(B)]. In the presence of 50% TFE, this band is strongly red-shifted to 203 nm [$[\theta] = 12,404 \text{ deg cm}^2 \text{dmol}^{-1}$], suggesting α/β (α -helix and/or β turn) populations or more structural organisation [Figure 3(B)]. From 20 to 60% of TFE, the intensity of the negative band

at ~ 204 nm fluctuates modestly between $-10,000 \text{ deg cm}^2 \text{dmol}^{-1}$ and $-15,000 \text{ deg cm}^2 \text{dmol}^{-1}$ [inset Figure 4(B)]. It should be noted that an increase in concentration of TFE has little effect on the structure. In the same context, a thermal unfolding study performed at 205 nm [Figure 5(A)] and 222 nm [Figure 5(B)], between 5 and 55 $^{\circ}\text{C}$, showed marginal changes. Such an observation is relevant to a stable conformational state. Thus, the amide-mediated cyclisation of peptide **3** exerts structuring and stabilising effects in TFE, which are in the favour of α/β populations.

In water, the CD spectrum of the peptide cyclised through RCM and possessing an unsaturated diether bridge (compound **7**) is typical for a random form [$[\theta] = -5908 \text{ deg cm}^2 \text{dmol}^{-1}$ at 197 nm, Figure 3(C)].

In the presence of 50% TFE, this peptide exhibits a red-shifted negative maximum at 204 nm [$[\theta] = -6,770 \text{ deg cm}^2 \text{dmol}^{-1}$] and a weak negative signal observed at ~ 223 nm [$[\theta] = -2,113 \text{ deg cm}^2 \text{dmol}^{-1}$, $n\pi^*$ transition, Figure 3(C)].

Recently, Manning and Woody have provided convincing simulation data concerning the 3_{10} -helix CD signature [33]. More precisely, they showed that 3_{10} -helix is characterised by an intense

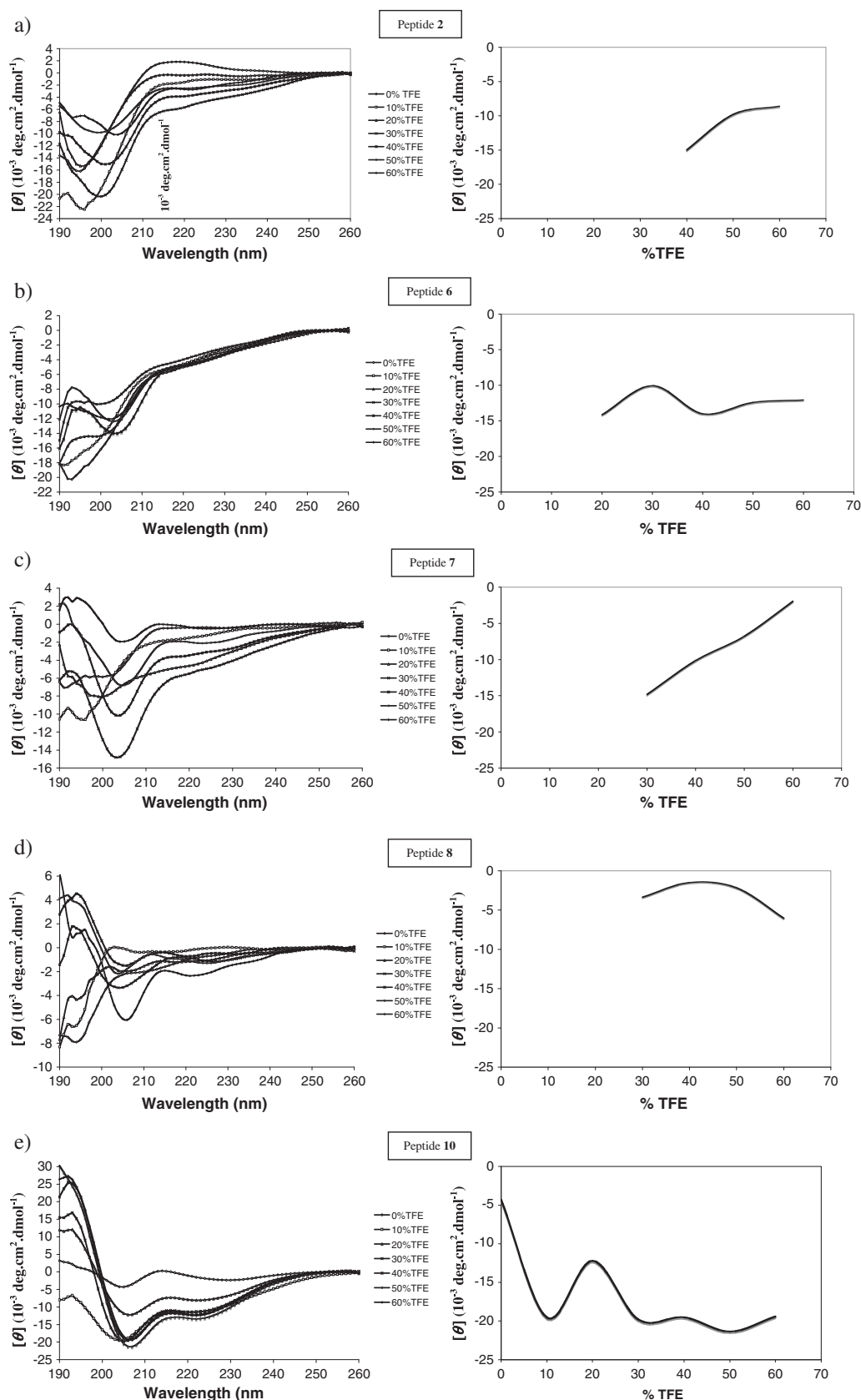


Figure 4. Spectra of the cyclized peptides in function of the amount of TFE (from 0 to 60% TFE, v:v) and evolution of the maximum MRE in function of the percentage of TFE: (a) peptide **2**, (b) peptide **6**, (c) peptide **7**, (d) peptide **8** and (e) peptide **10**. The mean residue ellipticity $[\theta]$, MRE values are expressed in 10^{-3} deg cm² dmol⁻¹. Inset: intensity of the negative maximum at 205 nm as a function of the percentage of TFE. We represent only the evolution of the signal for the red-shifted negative maximum, which is relevant to structuring events.

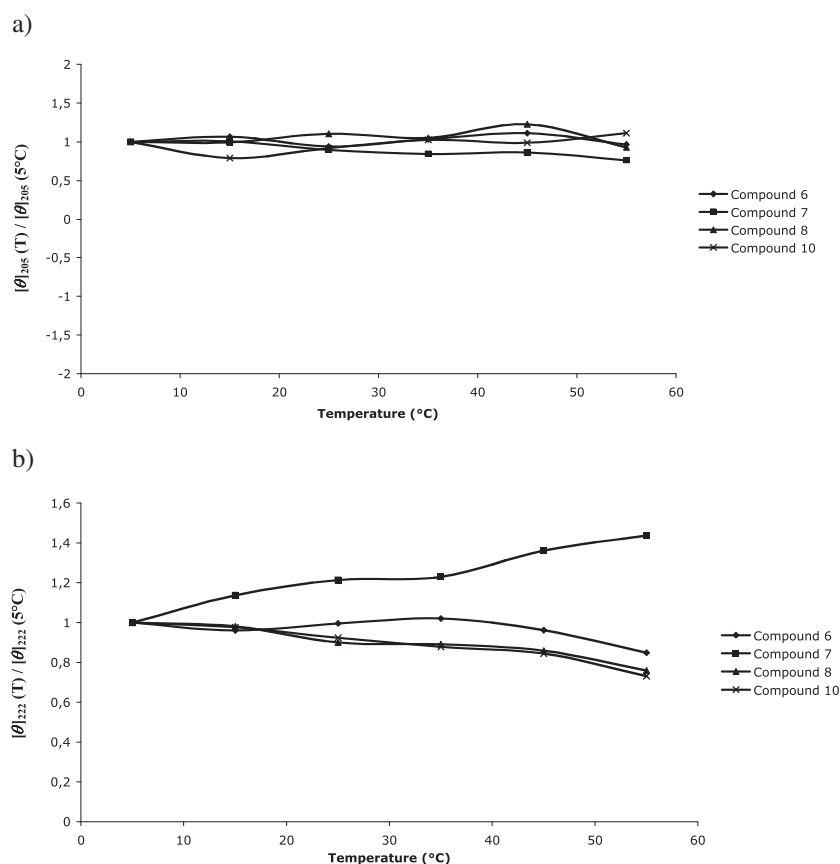


Figure 5. Unfolding of the secondary structures of the cyclised compounds **6**, **7**, **8** and **10** monitored at 205 (a) and 222 nm (b). The mean residue ellipticity $[\theta]$ values are expressed in 10^{-3} deg cm^2 dmol^{-1} .

208 nm band relative to the 222 nm band, in contrast with an α -helix [34]. Indeed, the α -helix is usually characterised by a strong positive maximum at ~ 190 nm and two negative bands at 208 nm and 222 nm. In 1996, Toniolo *et al.* proposed to use the ratio $R = [\theta]_{222} / [\theta]_{208}$ (i.e. $[\theta]_{\pi \rightarrow \pi^*} / [\theta]_{\pi \rightarrow \pi^*}$) to detect a 3_{10} -helix: $R \leq 0.4$ in the case of 3_{10} helix and $R \approx 1$ in the case of α -helix [35,34]. More precisely, the values would be $0.20 < R < 0.40$ in the case of 3_{10} helix and $0.85 < R < 0.90$ in the case of the α -helix [39,40]. The ratio $[\theta]_{222} / [\theta]_{205}$ value being of ~ 0.31 in our case, a 3_{10} helix for **7** seems likely [16,35,36]. As previously observed, the linear decrease of the intensity of the negative maximum at 204 nm with increasing amounts of TFE (from -15 deg cm^2 dmol^{-1} to -2 deg cm^2 dmol^{-1}) is relevant to a lack of cooperativity, and therefore, a redistribution of random population [inset Figure 4 (C)]. It is noteworthy that peptide populations are unchanged between 5 and 55 °C, as stressed by the measure of the ratio $[\theta]_{205}(T^{\circ}\text{C}) / [\theta]_{205}(5^{\circ}\text{C})$ [Figure 5(A)] and the ratio $[\theta]_{222}(T^{\circ}\text{C}) / [\theta]_{222}(5^{\circ}\text{C})$ [Figure 5(B)].

In water, the CD spectrum of **8** [Figure 3(D)], the compound in which the double bond has been reduced shows a CD profile similar to the one of its unsaturated precursor (peptide **7**), with a strong negative maximum at 194 nm $[\theta] = -7902$ deg cm^2 dmol^{-1} . In 50% TFE and with respect to the absorption bands intensities, the positive maximum at 192 nm $[\theta] = 4391$ deg cm^2 dmol^{-1} , $\pi\pi^*$ transition polarised perpendicular to the helix axis], the negative maximum (shoulder at 204 nm, $[\theta] = -2165$ deg cm^2 dmol^{-1} , $\pi\pi^*$ transition polarised parallel to the helix axis) and the negative shoulder at 225 nm $[\theta] = -1296$ deg cm^2 dmol^{-1} , $n\pi^*$ transition],

could be relevant to a 3_{10} helix [Figure 3(D)]. The study of the conformation of the derivative **8** as a function of the percentage of TFE reveals not only random forms but also helix contribution, as shown by the shoulder at 225 nm [inset Figure 4(D)]. By referring to the maximum at 204 nm, modest modifications of the absorbance at this wavelength were observed [Figure 4(D)]. However, the increase of the maximum at 191 nm when TFE increases confirms an enrichment of peptide populations adopting a helical form.

Next, we studied the CD signature of cyclopeptide **10**, which was obtained by the Cu-catalysed Huisgen cycloaddition reaction involving modified amino acid side chains, in this case, (*S*)-propargylglycine (Pra) in position 2 and (*S*)- ϵ -azido-norleucine (ϵN_3 -Nle) in position 6. In contrast to the lactam analogue (compound **6**), peptide **10** appears to be more structured and this as early as 0% TFE, as evidenced by the negative maximum at 205 nm [Figure 4(E)].

Remarkably, the behaviour of this peptide is different from the others. In contrast to the lactam (**6**) and the RCM derivatives (**7** and **8**), it is much more structured into 3_{10} helix as evidenced by the positive maximum at 192 nm, the negative maximum at 204 nm and the weak minimum at 222 nm [Figures 3(E) and 4(E)]. Accordingly, the ratio $[\theta]_{222} / [\theta]_{205}$ is approximately 0.60 and remains constant during titration [Figure 6(A)] [16, 34–36].

Thus, the triazole motif appears particularly important for peptide folding and stabilisation into 3_{10} helix. In agreement with this statement, a negative maximum near 205 nm ($\pi\pi^*$ transition) and a negative shoulder between 215 and 230 nm ($n\pi^*$ transition) were observed in the absence and in the presence of TFE, giving

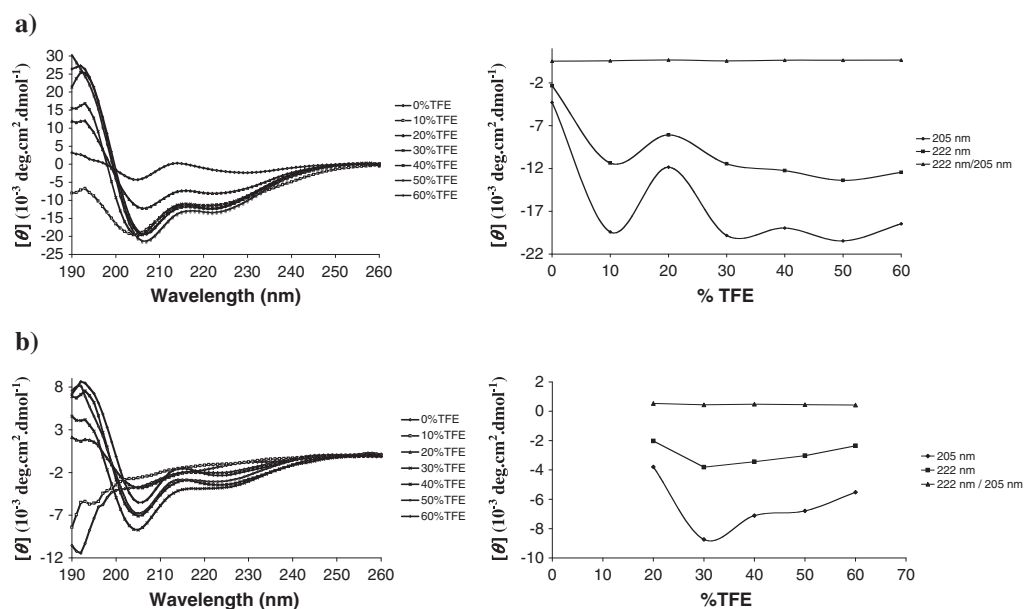


Figure 6. Intensity of the $[\theta]$ values (in $10^3 \text{ deg cm}^2 \text{ dmol}^{-1}$) recorded at ~ 205 and 222 nm for compounds **10** (a) and **9** (b). Inset: the ratio values $[\theta]_{222 \text{ nm}}/[\theta]_{205 \text{ nm}}$ has no unit.

substantial weight to a superior structural arrangement of the peptide, even in water [Figure 4(E)].

It is noteworthy that at 0 and 10% TFE **9** is random in contrast to the cyclised analogue. Starting from TFE percentages of 20%, a CD profile similar to **10**, with a positive maximum at $\sim 192 \text{ nm}$, a strong minimum near 205 nm and a negative band near 222 nm [Figure 6(B)], is exhibited by the linear precursor of the click cyclisation (i.e. H-Lys-Pra-Nle-Aib-Val- ϵ -N₃Nle-Lys-Tyr-NH₂, **9**). When compared with the CD spectra of peptide **10** [Figure 6(A)], the intensity of the bands recorded for **9** is systematically lower, an observation consistent with the fact that random populations participate in the signal at 205 nm . In view of the absorbance changes of the spectrum recorded for **2** and **6**, the spectral signature associated with **9** and **10** suggests also that the Pra and/or ϵ -N₃Nle functionalities aid in peptide folding [15].

Lastly, the ratio value of the mean residue ellipticities recorded at 205 and 222 nm shows that $R = [\theta]_{222}/[\theta]_{205} \sim 0.45$ and remains constant during titration, which is indicative of the presence of 3_{10} helix [Figure 6(B)] [16,34–36]. Note that cooperativity appears evident (inset), revealing a well-defined conformation distinct from random species.

Hence, the triazole-mediated cyclisation is not only associated with a helix-turn conformation, but it seems that the Pra and ϵ -N₃Nle side chains are involved in peptide folding in such a way that a structural organisation is quickly achieved. Accordingly, the ratio of the mean-residual ellipticity values recorded at 205 and 222 nm , as a measure of conformational changes, remains constant during titration with values around 0.60 [Figure 5(A)] [16,35,36].

Conclusions

This study has shown that in general, linear peptide analogues of a VIP octapeptide segment lose their helical propensity when taken out of an extended α -helix domain (cf. spectra of peptides

2–5 in water). In the presence of 50% TFE, random coil and minor secondary structure are observed. With regard to the cyclised peptides, one can conclude that the lactam analogue **6** also prefers random coil conformations in water but seems to adopt structured forms that are in favour of α -helix/ β -turn populations when the measurements were carried out in 50% TFE/water (v/v). Both analogues resulting from RCM cyclisation (i.e. compounds **7** and **8**) again show random conformations in water. The CD spectra of these compounds are, however, indicative of 3_{10} helix populations at high TFE content (50%). With respect to the linear precursor of the CuAAC reaction and the triazole-bridged peptide analogue (**9** and **10**, respectively), a higher propensity of folding is observed, as compared with the RCM and lactam peptides. Whereas the click precursor **9** seems to fold into a 3_{10} helix at a TFE content equal to 20% and higher, the triazole-tether stabilises the peptide **10** in that same conformation, even in the absence of TFE. As a result, we have obtained the following ranking of the different structural motifs for helix stabilisation: triazole tether > linear azide/alkyne precursor amide tether > RCM tethers. In consequence, the results are different from those in an earlier study that compared different strategies to stabilise the β -turn structure [19]. Although, these results clearly seem to be in favour of the Huisgen cycloaddition for helix stabilisation, the observations in this work might be sequence dependant. The remarkable folding propensity of the linear azide/alkyne analogue **9** prompts us to investigate the generality of this observation more in depth.

Acknowledgements

The work of SB, DT and CB was supported by a collaboration convention between the Ministère du Développement économique, de l'Innovation et de l'Exportation du Québec (MDEIE) and the Fund for Scientific Research Flanders (FWO Vlaanderen) (FWO G.A055.10 N and PSR-SIIRI-417). The work of YJ was supported by the Centre National pour la Recherche Scientifique (CNRS), the University Pierre et Marie Curie and the Ecole Normale Supérieure.

References

- 1 Guharoy M, Chakrabarti P. Secondary structure based analysis and classification of biological interfaces: identification of binding motifs in protein-protein interactions. *Bioinformatics* 2007; **23**: 1909–1918. DOI: 10.1093/bioinformatics/btm274
- 2 Guharoy M, Chakrabarti P. Empirical estimation of the energetic contribution of individual interface residues in structures of protein-protein complexes. *J. Comput. Aided Mol. Des.* 2009; **23**(9): 645–654. DOI: 10.1007/s10822-009-9282-3
- 3 Vlieghe P, Lisowski V, Martinez J, Khrestchatsky M. Synthetic therapeutic peptides: science and market. *Drug Discov. Today* 2010; **15**: 40–56. DOI: 10.1016/j.drudis.2009.10.009
- 4 Katsara M, Tselios T, Deraos S, Deraos G, Matsoukas MT, Lazoura E, Matsoukas J, Apostopoulos V. Round and round we go: cyclic peptides in disease. *Curr. Med. Chem.* 2006; **13**: 2221–2232. DOI:10.2174/092986706777935113
- 5 White CJ, Yudin AK. Contemporary strategies for peptide macrocyclization. *Nature Chem.* 2011; **3**: 509–524. DOI: 10.1038/nchem.1062
- 6 Driggers EM, Hale SP, Lee J, Terret NK. Macrocycles for drug discovery. An underexploited structural class. *Nature Rev. Drug. Disc.* 2008; **7**: 608–624. DOI: 10.1038/nrd2590
- 7 Kelso MJ, Hoang HN, Oliver WV, Sokolenko N, March DR, Appleton TG, Fairlie DP. A cyclic metalloprotein induce alpha helicity in short peptide fragments of thermolysin. *Angew. Chem. Int. Ed.* 2003; **42**: 421–424. DOI: 10.1002/anie.200390128
- 8 Garner J, Harding MM. Design and synthesis of α -helical peptides and mimetics. *Org. Biomol. Chem.* 2007; **5**: 3577–3585. DOI: 10.1039/B710425A
- 9 Davis JM, Tsou LK, Hamilton AD. Synthetic non-peptide mimetics of α -helices. *Chem. Soc. Rev.* 2007; **36**: 326–334. DOI: 10.1039/B608043J
- 10 Walensky LD, Kung AL, Escher I, Malia TJ, Barbutto S, Wright RD, Wagner G, Verdine GL, Korsmeyer SJ. Activation of apoptosis *in vivo* by a hydrocarbon-stapled BHL Helix. *Science* 2004; **305**: 1466–1470. DOI: 10.1126/science.1099191
- 11 Verdine GL, Hilinski GJ. Stapled peptides for intracellular drug targets. *Meth. Enzymol.* 2012; **503**: 3–33. DOI: 10.1016/B978-0-12-396962-0.00001-X
- 12 Scrima M, Le Chevalier-Isaad A, Rovero P, Papini AM, Chorev M, D'Ursi AM. Cu^I-catalyzed azide-alkyne intramolecular *i*-to-(*i*+4) side-chain-to-side-chain cyclization promotes the formation of helix-like secondary structures. *Eur. J. Org. Chem.* 2010; 446–457. DOI: 10.1002/ejoc.200901157
- 13 Yoshida M, Mori A, Kotani E, Oka M, Makino H, Fujita H, Ban J, Ikeda Y, Kawamoto T, Goto M, Kimura H, Baba A, Yasuma T. Discovery of novel and potent orally active calcium-sensing receptor antagonists that stimulate pulsatile parathyroid hormone secretion: synthesis and structure-activity relationships of tetrahydropyrazolopyrimidine derivatives. *J. Med. Chem.* 2011; **54**: 1430–1440. DOI: 10.1021/jm101452x
- 14 Kawamoto SA, Coleska A, Ran X, Yi H, Yang CY, Wang S. Design of triazole-stapled BCL9 α -helical peptides to target the β -Catenin/B-Cell CLL/lymphoma 9 (BCL9) protein-protein interaction. *J. Med. Chem.* 2012; **55**: 1137–1146. DOI: 10.1021/jm201125d
- 15 Harrison RS, Ruiz-Gomez G, Hill TA, Chow SY, Shepherd NE, Lohman RJ, Abbenante G, Hoang HN, Fairlie DP. Novel helix-constrained nociceptin derivatives are potent agonists and antagonists of ERK phosphorylation and thermal analgesia in mice. *J. Med. Chem.* 2010; **53**:8400–8408. DOI: 10.1021/jm101139f
- 16 Blackwell HE, Grubbs RH. Highly efficient synthesis of covalently cross-linked peptide helices by ring-closing metathesis. *Angew. Chem. Int. Ed.* 1998; **37**: 3281–3284. DOI: 10.1002/(SICI)1521-3773(19981217)37:23 < 3281::AID-ANIE3281 > 3.0.CO;2-V
- 17 Schafmeister CE, Po J, Verdine GL. An all-hydrocarbon cross-linking system for enhancing the helicity and metabolic stability of Peptides. *J. Am. Chem. Soc.* 2000; **122**: 5891–5892. DOI: 10.1021/ja000563a
- 18 Onoue S, Matsumoto A, Nagano Y, Ohshima K, Ohmori Y, Yamada S, Kimura R, Yajima T, Kashimoto K. α -Helical structure in the C-terminus of vasoactive intestinal peptide: functional and structural consequences. *Eur. J. Pharmacol.* 2004; **485**: 307–316. DOI: 10.1016/j.ejphar.2003.11.046; Nicole P, Lins L, Rouyer-Fessard C, Drouot C, Fulcrand P, Thomas A, Couvineau A, Martinez J, Brasseur R, Laburthe M. Identification of key residues for interaction of vasoactive intestinal peptide with human VPAC1 and VPAC2 receptors and development of a highly selective VPAC1 receptor agonist. *J. Biol. Chem.* 2000; **275**: 24003–24012. DOI:10.1074/jbc.M002325200
- 19 Larregola M, Lequin O, Karoyan P, Guianvarc'h D, Lavielle S. β -Amino acids containing peptides and click-cyclized peptide as β -turn mimics: a comparative study with 'conventional' lactam- and disulfide-bridged hexapeptides. *J. Pept. Sci.* 2011; **17**: 632–643. DOI: 10.1002/psc.1382
- 20 Seebach D, Gardiner J. β -Peptidic peptidomimetics. *Acc. Chem. Res.* 2008; **41**: 1366–1375. DOI: 10.1021/ar700263g
- 21 Cammers-Goodwin A, Allen TJ, Oslick SL, McClure KF, Lee JH, Kemp DS. Mechanism of stabilization of helical conformations of polypeptides by water containing trifluoroethanol. *J. Am. Chem. Soc.* 1996; **118**: 3082–3090. DOI: 10.1021/ja952900z
- 22 Luo P, Baldwin RL. Mechanism of helix induction by trifluoroethanol: a framework for extrapolating the helix-forming properties of peptides from trifluoroethanol/water mixtures back to water. *Biochemistry* 1997; **36**: 8413–8421. DOI: 10.1021/bi9707133
- 23 Skwierawska A, Oldziej S, Liwo A, Scheraga HA. Conformational studies of the C-terminal 16-amino-acid-residue fragment of the B3 domain of the immunoglobulin binding protein G from streptococcus. *Biopolymers* 2009; **91**: 37–51. DOI: 10.1002/bip.21080
- 24 Jasanoff A, Fersht AR. Quantitative determination of helical propensities from trifluoroethanol titration curves. *Biochemistry* 1994; **33**: 2129–2135. DOI: 10.1021/bi00174a020
- 25 Woody RW. Studies of theoretical circular dichroism of polypeptides: contributions of beta-turns. *Peptides, Polypeptides and Proteins*, Blout ER, Bovey FA, Goodman M and Lotan N (Eds). New-York: John Wiley & Sons, 1974; 338–350.
- 26 Platt JR. Classification of spectra of cata-condensed hydrocarbons. *J. Chem. Phys.* 1949; **17**: 484–495. DOI: 10.1063/1.1747293
- 27 Kleven HB, Platt JR. Spectral resemblances of cata-condensed hydrocarbons. *J. Chem. Phys.* 1949; **17**: 470–481. DOI: 10.1063/1.1747291
- 28 Wollmer A, Fleischhauer J, Strassburger W, Thiele H, Brandenburg D, Dodson G, Mercola D. Side-chain mobility and the calculation of tyrosyl circular dichroism of proteins. Implications of a test with insulin and des-B1-phenylalanine insulin. *Biophys. J.* 1977; **20**: 233–243. DOI:10.1016/S0006-3495(77)85546-X
- 29 Woody RW, Dunker AK. Aromatic and cystine side-chain circular dichroism in proteins. *Circular Dichroism and the Conformational Analysis of Biomolecules*, Fasman GD (Eds). New York and London: Plenum, 1996; 109–157.
- 30 Vijayakumar EKS, Balam P. Stereochemistry of α -aminoisobutyric acid peptides in solution: helical conformations of protected dipeptides with repeating Aib-L-Ala and Aib-L-Al sequences. *Biopolymers* 1983; **22**: 2133–2140. DOI: 10.1002/bip.360220911
- 31 Zhang L, Hermans J. 3_{10} versus α -helix: a molecular dynamics study of the conformational preferences of Aib and alanine. *J. Am. Chem. Soc.* 1994; **116**: 11915–11921. DOI: 10.1021/ja00105a034
- 32 Raghothama S, Chaddha M, Balam P. Determination of Aib residue conformation in peptides using diagnostic sidechain-backbone nuclear Overhauser effects. *Proc. Natl. Acad. Sci. India* 1996; **66**: 33–44
- 33 Manning MC, Woody RW. Theoretical CD studies of polypeptides helices: examination of important electronic and geometric factors. *Biopolymers* 1991; **31**: 569–586. DOI: 10.1002/bip.360310511
- 34 Hammerström JGT, Gauthier TJ, Hammer RP, McLaughlin ML. Amphipathic control of the 3_{10} - α -helix equilibrium in synthetic peptides. *J. Pept. Res.* 2001; **58**: 108–116. DOI: 10.1034/j.1399-3011.2001.00858.x
- 35 Toniolo C, Polese A, Formaggio F, Crisma M, Kamphuis J. Circular dichroism spectrum of a Peptide 3_{10} -helix. *J. Am. Chem. Soc.* 1996; **118**: 2744–2745. DOI: 10.1021/ja9537383
- 36 Blackwell HE, Sadowsky JD, Howard RJ, Sampson JN, Chao JA, Steinmetz WE, O'Leary DJ, Grubbs RH. Ring-closing metathesis of olefinic peptides: design, synthesis, and structural characterization of macrocyclic helical peptides. *J. Org. Chem.* 2001; **66**: 5291–5302. DOI: 10.1021/jo015533k
- 37 Sharma GVM, Yadav TA, Choudhary M, Kunwar AC. Design of β -amino acid with backbone-side chain interactions: stabilization of 14/15 helix in α/β -peptides. *J. Org. Chem.* 2012; **77**: 6834–6848. DOI: 10.1021/jo300865d
- 38 Hayen A, Schmitt MA, Ngassa FN, Thomasson KA, Gellman SH. Two helical conformations from a single foldamer backbone: "split personality" in short α/β -peptides. *Angew. Chem. Int. Ed.* 2004; **43**: 505–510. DOI: 10.1002/anie.200352125
- 39 Moretto A, Formaggio F, Kaptein B, Broxterman QB, Wu L, Keiderlig TA, Toniolo C. First homo-peptides undergoing a reversible 3_{10} - α -helix transition: critical main-chain length. *Biopolymers Pept. Sci.* 2008; **90**: 567–574. DOI: 10.1002/bip.21016
- 40 Caporale A, Sturlese M, Gesiot L, Zanta F, Wittelsberger A, Cabrelle C. Side Chain cyclization based on serine residues: synthesis, structure, and activity of a novel cyclic analogue of the parathyroid hormone fragment 1–11. *J. Med. Chem.* 2010; **53**: 8072–8079. DOI: 10.1021/jm1008264